NANO LETTERS

2006
Vol. 6, No. 4
843−847

Continuous Distribution of Emission States from Single CdSe/ZnS Quantum Dots

Kai Zhang,[†] Hauyee Chang,[†,‡] Aihua Fu,[†] A. Paul Alivisatos,[†,§] and Haw Yang*[,†,||]

Department of Chemistry, University of California at Berkeley, and Materials Sciences Division and Physical Biosciences Division, Lawrence Berkeley National Laboratory, Berkeley, California 94720

Received March 1, 2006

ABSTRACT

The photoluminescence dynamics of colloidal CdSe/ZnS/streptavidin quantum dots were studied using time-resolved single-molecule spectroscopy. Statistical tests of the photon-counting data suggested that the simple "on/off" discrete state model is inconsistent with experimental results. Instead, a continuous emission state distribution model was found to be more appropriate. Autocorrelation analysis of lifetime and intensity fluctuations showed a nonlinear correlation between them. These results were consistent with the model that charged quantum dots were also emissive, and that time-dependent charge migration gave rise to the observed photoluminescence dynamics.

Colloidal semiconductor nanocrystals, or quantum dots (QDs), have been the focus of much research effort in the past decade. The development of these colloidal dots has allowed the concepts of quantum confinement and dimensional control of electronic and optical properties to find entirely new areas of application, for instance in fluorescent labeling of biological specimens. At the single-particle level, however, colloidal QDs exhibit surprisingly complicated time-dependent behavior in their photoluminescence (PL) characteristics.

The first report of PL *on*−*off* intermittency from individual QDs attributed the *off* period in a PL time trace to a photoionized, charged state, and the *off*-to-*on* process to reneutralization of the particle.[1] QD PL suppression by photoionization is thought to result from an Auger-assisted process.[2] This picture of photon-assisted charging was confirmed by direct measurement of particle charges using electrostatic force microscopy.[3,4] The precise nature of the charged state, however, remains unclear. The formation and stabilization of charges in ZnS capped CdSe core−shell QDs may involve electrons or holes that are trapped in states at the surface of the CdSe core or at the surface of the ZnS shell.[5,6] Relocation of the external charge is thought to cause the emission spectrum to vary with time.[7]

Statistical analyses of PL time trajectories from single QDs provide further insight into the underlying dynamics. Within the two-state framework, both the *on*- and *off*-state resident times were found to exhibit a power-law distribution which, in turn, may imply either an exponential distribution of trap depths or a dynamically varying rate of reneutralization.[8,9] To explain the prolonged *on* time, the neutral-*on* and charged-*off* two-state model was recently extended to a three-state model, permitting PL from a charged state where the charge is trapped far away from the core.[10] Taking together the notion that charged QDs are also emissive and that there exists a distribution of surface charge traps, one would expect that location of surface charges should affect the emission intensities[11] such that they are not strictly *on* and *off*.

A schematic configuration for single-molecule optical experiments is illustrated in Figure 1. Qdot655 streptavidin conjugates from Quantum Dot Corp. (now Invitrogen, 1002-1, lot no. 0104-0034) were used in this study. These QDs were comprised of a core of CdSe capped by a layer of ZnS. This core−shell material is further coated with a polymer shell that allows conjugation of streptavidin. Transmission electron microscopy (TEM) characterization of the morphology for the same sample lot used in this study showed that the average length, width, and aspect ratio were 11.9 ± 2.3 nm (19%), 6.95 ± 0.88 nm (13%), and 1.72 ± 0.37 (22%), respectively (cf. Figure 1, inset B). Included in the parentheses are relative standard deviations. These TEM results indicate that shape variations in individual QDs cannot be ruled out in explaining the results from individual QDs.

The evaluation of single molecule trajectories can be dramatically influenced by the time scale of binning (see Figure 2 for an example of how a distribution of intensity

[†] Department of Chemistry, University of California at Berkeley.
[‡] Current address: Xradia Inc., Concord, CA.
[§] Materials Sciences Division, Lawrence Berkeley National Laboratory.
[||] Physical Biosciences Division, Lawrence Berkeley National Laboratory.

10.1021/nl060483q CCC: $33.50
Published on Web 03/21/2006

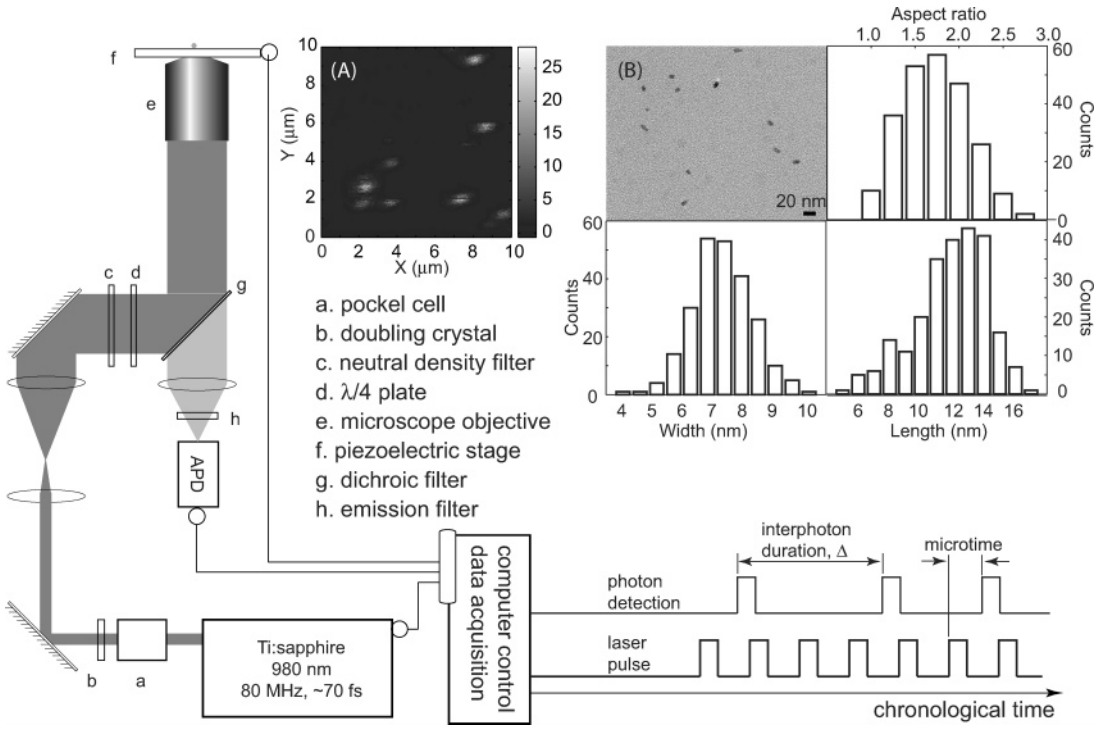

Figure 1. Schematic of the single-molecule microscope and TCSPC photon registration scheme. Inset A shows a representative image of single QDs, where blinking during raster scanning is evident (the dark, horizontal lines within each bright spot). Inset B is a representative TEM image of the CdSe/ZnS/streptavidin quantum dots. Distributions of crystal length, width, and aspect ratio counted from more than 200 QDs are also shown. For each detection event, the time period between two sequentially detected photons (the interphoton duration, Δ) and the time lapse between the excitation pulse and the detection of luminescence photon (the microtime) are recorded and stored in a computer for later data analysis.

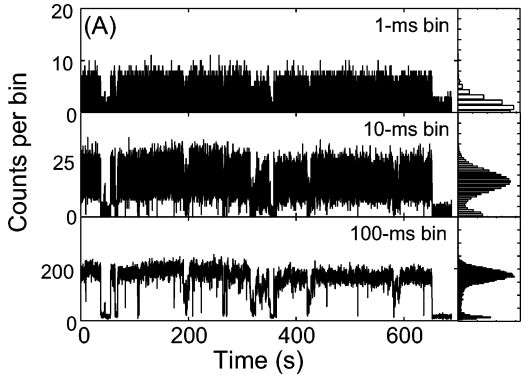

Figure 2. A 11-min time-resolved trajectory of a single QD at various bin times, illustrating how statistical characteristics are affected by the choice of bin times. For example, shown on the right of each time trace is the corresponding intensity histogram, the shape of which apparently changes with bin time. The data were taken using a time-stamped time-correlated single-photon counting setup (cf. Figure 1).

levels can be obscured by binning artifacts). The recently developed changepoint method provides a statistically unbiased and systematic method for analyzing such trajectories.[12] In this method, the time instances at which the emission intensity changes are accurately determined, one photon at a time, using a log-likelihood ratio test, to reveal new features such as intensity levels and fast transitions that are likely to be blurred by binning. Bayesian information criteria are employed to determine the number of discrete intensity levels that are supported by the experimental data. Here we apply this method to single QD photon emission trajectories, to determine the nature of the intensity distributions.

The changepoint reconstructed intensity and lifetime trajectories for the QD in Figure 2 are shown in Figure 3. Visually, the reconstructed trajectory follows the binned raw photon data very well. To assess the extent to which dynamical information is recovered, fluctuation correlation of 100-μs binned trajectory is compared with that of changepoint reconstructed trajectory. Figure 4A shows that dynamics from 1.8 ms to the length of the entire trajectory (688 s) are quantitatively recovered. The relatively slowly varying time-correlation curve on the 2-ms to 1-s time scales (cf. Figure 4) is indicative of a prolonged bright state. This is in agreement with the model for ZnS capped CdSe QDs proposed by Verberk et al.,[10] who extended the two-state model (neutral-*on* and charged-*off*) to permit PL from a charged state if the charge is trapped far away from the CdSe core. The trapped charge in the emissive state frustrates further photoionization via a Coulomb-blockade mechanism, thereby allowing for a prolonged *on* state.

The luminescence lifetime in each changepoint determined intensity segment can also be estimated[14] and appears to be positively correlated with the emission intensity (cf. Figure 3), indicative of dynamical quenching pathways.[15,16] More quantitative evaluation is made by comparing their respective correlation functions. As illustrated in Figure 4, the intensity and lifetime fluctuations exhibit significant differences on time scales greater than 17 ms. To examine if the discrete-

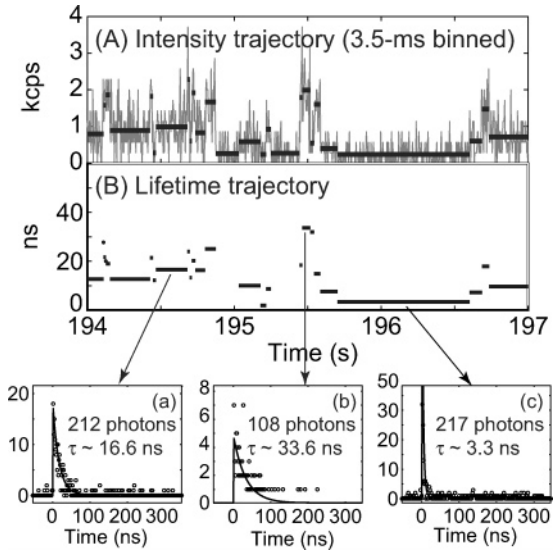

Figure 3. (A) Typical result of changepoint reconstruction (with 95% confidence) for time-dependent emission intensity from a single QD. The 3.5-ms binned intensity trace is shown in gray and the reconstructed one as thick horizontal segments. Note those fast transitions that are otherwise obscured by photon counting noise are successfully recovered. (B) Luminescence lifetime from each changepoint segment. Subpanels a−c: Representative microtime histograms for different luminescence lifetimes (○), in which the maximum likelihood fits are overlaid as solid lines.

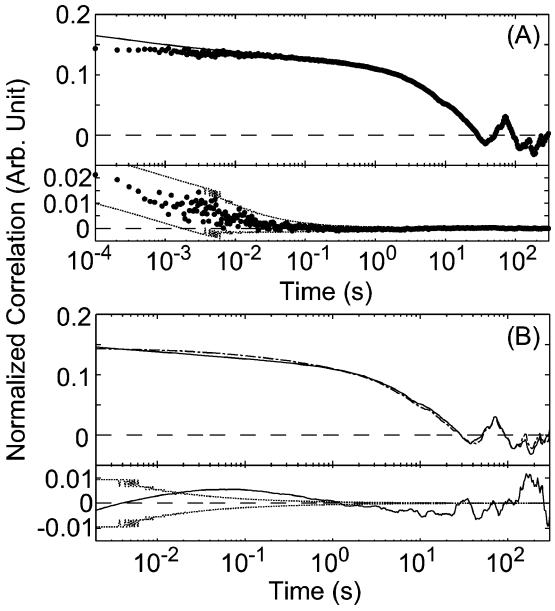

Figure 4. (A) Comparison of intensity fluctuation correlation of photon-counting trajectory (●) with that of changepoint recovered trajectory (—). The zoomed difference trajectory is displayed at the bottom where the 95% error bounds (···) indicate that information of intensity dynamics greater than 1.8 ms is quantitatively recovered. The correlation curve appears relatively flat at short times, similar to those that have been reported for ZnS capped CdSe nanocrystals.[13] (B) Comparison of intensity (—) and lifetime (· − ·) fluctuation correlations of the changepoint-recovered trajectory. While the faster dynamics (<17 ms) of emission intensity and luminescence lifetime appear indistinguishable with 95% confidence (···), they are clearly different at longer times. The QD shown in Figure 2 is used for this figure.

state model is suitable for describing the emission behavior of single QD, we first find the most likely number of intensity states that is supported by experimental data using the Bayesian information criterion (BIC)[12]

$$\mathrm{BIC} = 2\mathcal{L}_{\mathrm{G}} - (2n_{\mathrm{G}} - 1)\ln N_{\mathrm{cp}} - N_{\mathrm{cp}} \ln N$$

where N_{cp} is the number of intensity change points, N is the number of photons contained in the trajectory, and $\mathcal{L}_{\mathrm{G}}$ is the log-likelihood which evaluates how closely the n_{G}-state reconstructed intensity trajectory matches the original data. The most likely minimum number of states that describe the experimental time trace is $n_{\mathrm{G}}^{\max}$ that maximizes BIC. For example, the QD shown in Figure 3 is found to be best described by as few as three distinct states. While the number of states determined by BIC analysis varies from particle to particle, we found it generally true that a simple two-state model is inadequate for describing the photophysics of a single QD.

To investigate if photons within each BIC categorized intensity group arise from the same emission state, we examine the exponentiality of interphoton duration using a Kolmogorov−Smirnov test.[17] The hypothesis that the distribution is exponential is rejected with an error rate of α if

$$D = \max_{1 \le m \le n} \{|F^*(\Delta_m) - S_n(\Delta_m)|\} > \epsilon_\alpha$$

where $F^*(\Delta_m) = \int_0^{\Delta_m} (1/\bar{\Delta})\ \mathrm{e}^{(-\Delta/\bar{\Delta})}\ \mathrm{d}\Delta$ is the cumulative exponential distribution function with $\bar{\Delta} = 1/n\sum_{m=1}^{n} \Delta_m$, and $S_n(\Delta_m) = m/n$ is the sample cumulative sum of ordered interphoton durations $\{\Delta_1 \le \cdots \le \Delta_m \le \cdots \le \Delta_n\}$. In the current work, α is chosen to be 1% and the critical value is computed using $\epsilon_\alpha \simeq 1.25/N^{1/2}$ for $N \le 10\,000$. This simplified test allows one to rapidly assess the confidence level for the assignment of a discrete state or of a continuous distribution, thereby placing visual examination (cf. Figure 5) on a statstically more robust footing. As an example of this test, results for the QD on Figure 2 are summarized in Table 1, suggesting that photons within each BIC group do not arise from a single state with the same emission intensity. This conclusion leads us to consider an alternative scenario where the emission state is continuously distributed and evolves with time.

To further characterize single QDs, we construct probability distributions of emission intensity ($\hat{I}$) and luminescence lifetime ($\hat{\tau}$), as well as their joint distribution function, fluorescence lifetime−intensity distribution (FLID) map for each QD

$$P(\hat{I}, \hat{\tau}) = \sum_i \frac{1}{2\pi\hat{\sigma}_{I_i}\hat{\sigma}_{\tau_i}} \exp\left[-\frac{(I - \hat{I}_i)^2}{2\hat{\sigma}_{I_i}{}^2}\right] \exp\left[-\frac{(\tau - \hat{\tau}_i)^2}{2\hat{\sigma}_{\tau_i}{}^2}\right]$$

where $\hat{\sigma}_{I_i}^2$ and $\hat{\sigma}_{\tau_i}^2$ are respectively the expected variance for intensity and lifetime in the ith changepoint segment. As an example, the QD shown in Figure 2 is analyzed in Figure

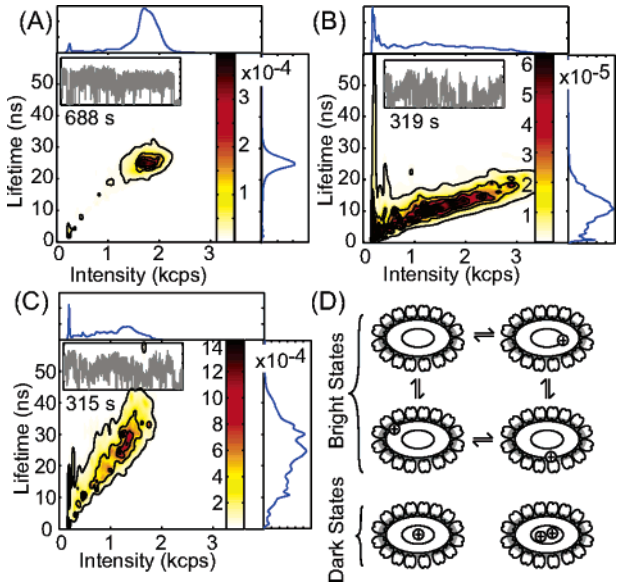

Figure 5. (A−C) Representative fluorescence lifetime−intensity distribution (FLID) of QDs. (A) is the QD shown in Figure 2. The overall intensity distribution is shown on the top panel while that of lifetime distribution is on the right panel. Darker color represents longer dwelling time. A 50-ms binned photon trajectory is also displayed in the inset as reference. The contour lines are for eye guides only. (D) Illustration for the formation of a continuous distribution of bright states. Photoionization induced charge can migrate between different surface trapping sites. These charged states where the positive trapping sites are away from the core, can still emit photons when excited, giving rise to various PL intensity. The QD switches to a dark state when the charge stays at the center of the QD, or when there are multiple charges such that nonradiative recombination becomes the dominant relaxation path.[10]

Table 1. Kolmogorov−Smirnov Test of Exponentiality for Every 10 000 Photons in the Time Trajectories[a]

state	N	n	I (counts/s)	D	$\epsilon_{0.01}$
QD1	956749	10000	1806	0.0151	0.0125
QD2	78690	10000	1089	0.0176	0.0125
QD3	17784	10000	206	0.0399	0.0125

[a] N is the total number of photons found in each state, n is the number of photons used in each exponentiality test, I is the average intensity of that BIC state. QD1, QD2, and QD3 are the intensity states for QD. These assignments are based on the BIC-grouped analysis.

5A. The top panel displays the overall $\hat{I}$ distribution, which roughly exhibits two clusters. The lower-intensity cluster peaks at ∼240 counts/s whereas the high-intensity one peaks at ∼1700 counts/s with significantly more weight. This is expected by visual examination of the raw trajectory, which indicates that this particular QD spends significantly more time on the "bright" state than on the "dark" state. There is, however, finite probability of finding this particle at intermediate intensity levels. While QDs have been shown to possess a permanent dipole,[18] it is unlikely that the observed intensity distribution arises from dipole reorientation because the overall polarization effect from our experimental setup is about 10%, much less than observed intensity variations.

Turning to the emission lifetime, $\hat{\tau}$, its distribution on the right panel appears to cluster around ∼25 ns, consistent with the ∼20-ns room-temperature PL lifetime measurements of high-intensity states.[15,16,19] The correlation between $\hat{I}$ and $\hat{\tau}$ is visualized by the FLID map displayed in Figure 5. In the range between $\hat{I} = 240$ counts/s and $\hat{I} = 1500$ counts/s, $\hat{\tau}$ appears to depend linearly on $\hat{I}$. At higher intensities (∼1500 counts/s $\leq \hat{I} \leq$ ∼2100 counts/s), however, $\hat{\tau}$ appears to fluctuate around $\hat{\tau} = 25$ ns instead of following the same linear trend. This observation is consistent with the time-correlation analysis in Figure 4, which shows that dynamics of PL lifetime are quantitatively different from those of intensity fluctuations.

In general, both the luminescence lifetime and emission intensity are distributed continuously (cf. Figure 5A−C). Higher-intensity states tend to exhibit longer luminescence lifetimes, whereas lower-intensity states exhibit shorter lifetimes. There is, however, no obvious linear relationship between lifetime and intensity. For example, in parts A and B of Figure 5, the $\hat{\tau}/\hat{I}$ slope gradually decreases at higher intensities. For some particles, on the other hand, the slope becomes steeper at higher intensities as shown in Figure 5C. Overall, there exists a wide distribution of FLID patterns which vary from particle to particle. This, in turn, suggests that FLID can be an effective tool to unravel the characteristics of individual particles or molecules in general.

Our analysis of experimental results suggests that PL intermittency of a single QD is inconsistent with discrete-state models. Instead, single QD PL should be considered as emanating from a distribution of emissive states, giving rise to the observed broad intensity distribution. While mechanisms including photoinduced reorganization of molecular absorbates at the surface,[20] and photooxidation related shape changes[21] may also be operative, here we rationalize the experimental observation generalizing the model proposed by Verberk et al. to allow the characteristics of the charge trapping state to vary as a function of time (cf. Figure 5D). The trapped charge is expected to modify the electronic structure of the QD,[11] likely to cause changes in the absorption cross section and radiative lifetime. As a result, both the radiative and nonradiative decay rates may change as a function of time to give rise to the broad, time-varying intensity distribution and distinct fluctuations in intensity and lifetime. The broad distribution in emission intensity can be understood as resulting from a distribution of positive charge traps at the core−shell interface, or at the shell−streptavidin layer. Over time, the charged QD may reneutralize but is quickly photoionized under the excitation laser illumination, or the charge may persist but migrate among the localized trapping states, likely via a thermally activated process.[22] Electrostatic force microscopy (EFM) shows single CdSe nanocrystal can devolop a positive charge upon exposure to weak, ambient light. Measurements taken during photoexcitation show photoionization of individual nanocrystals.[4] A fundamental understanding of the PL dynamiacs from a single QD could eventually provide clues for a rational design of nanostructures with tailored optical properties.[23]

Acknowledgment. We thank Professor E. Sánchez for the generous gift of a scanning program. H.Y. acknowledges financial support from the Office of Science, U.S. Depart-

ment of Energy, under Contract DE-AC03-76SF00098, from the National Science Foundation, and from the University of California at Berkeley. A.P.A. acknowledges support by NIH National Center for Research Resources through the University of California, Los Angeles, subaward agreement 0980GCD709 through the U.S. Department of Energy under Contract No. DE-AC03-76SF00098, and by DOD Advanced Research Project Agency under award No. 066995.

Supporting Information Available: Materials, descriptions of experimental details, and data analysis algorithms. This material is available free of charge via the Internet at http://pubs.acs.org.

References

(1) Nirmal, M.; Dabbousi, B. O.; Bawendi, M. G.; Macklin, J. J.; Trautman, J. K.; Harris, T. D.; Brus, L. E. *Nature* **1996**, *383*, 802−804.
(2) Efros, A. L.; Rosen, M. *Phys. Rev. Lett.* **1997**, *78*, 1110−1113.
(3) Krauss, T. D.; Brus, L. E. *Phy. Rev. Lett.* **1999**, *83*, 4840−4843.
(4) Krauss, T. D.; O'Brien, S.; Brus, L. E. *J. Phys. Chem. B* **2001**, *105*, 1725−1733.
(5) Rodríguez-Viejo, J.; Mattoussi, H.; Heine, J. R.; Kuno, M. K.; Michel, J.; Bawendi, M. G.; Jensen, K. F. *J. Appl. Phys.* **2000**, *87*, 8526−8534.
(6) Wang, X.; Qu, L.; Zhang, J.; Peng, X.; Xiao, M. *Nano Lett.* **2003**, *3*, 1103−1106.
(7) Neuhauser, R. G.; Shimizu, K. T.; Woo, W. K.; Empedocles, S. A.; Bawendi, M. G. *Phy. Rev. Lett.* **2000**, *85*, 3301−3304.
(8) Kuno, M.; Fromm, D. P.; Hamann, H. F.; Gallagher, A.; Nesbitt, D. J. *J. Chem. Phys.* **2001**, *115*, 1028−1040.
(9) Shimizu, K. T.; Neuhauser, R. G.; Leatherdale, C. A.; Empedocles, S. A.; Woo, W. K.; Bawendi, M. G. *Phys. Rev. B* **2001**, *63*, 205316.
(10) Verberk, R.; Oijen, A. M. v.; Orrit, M. *Phys. Rev. B* **2002**, *66*, 233202.
(11) Franceschetti, A.; Zunger, A. *Phys. Rev. B* **2000**, *62*, R16287−R16290.
(12) Watkins, L. P.; Yang, H. *J. Phys. Chem. B* **2005**, *109*, 617−628.
(13) Messin, G.; Hermier, J. P.; Giacobino, E.; Desbiolles, P.; Dahan, M. *Opt. Lett.* **2001**, *26*, 1891−1893.
(14) Brand, L.; Eggeling, C.; Zander, C.; Drexhage, K. H.; Seidel, C. A. M. *J. Phys. Chem. A* **1997**, *101*, 4313−4321.
(15) Schlegel, G.; Bohnenberger, J.; Potapova, I.; Mews, A. *Phys. Rev. Lett.* **2002**, *88*, 137401.
(16) Fisher, B. R.; Eisler, H.-J.; Stott, N. E.; Bawendi, M. G. *J. Phys. Chem. B* **2004**, *108*, 143−148.
(17) Lilliefors, H. W. *J. Am. Stat. Assoc.* **1969**, *64*, 387−389.
(18) Blanton, S. A.; Leheny, R. L.; Hines, M. A.; Guyot-Sionnest, P. *Phys. Rev. Lett.* **1997**, *79*, 865−868.
(19) Crooker, S. A.; Barrick, T.; Hollingsworth, J. A.; Klimov, V. I. *Appl. Phys. Lett.* **2003**, *82*, 2793−2795.
(20) Jones, M.; Nedeljkovic, J.; Ellingson, R. J.; Nozik, A. J.; Rumbles, G. *J. Phys. Chem. B* **2003**, *107*, 11346−11352.
(21) Sark, W. G. J. H. M. v.; Frederix, P. L. T. M.; Bol, A. A.; Gerritsen, H. C.; Meijerink, A. *ChemPhysChem* **2002**, *3*, 871−879.
(22) Banin, U.; Bruchez, M.; Alivisatos, A. P.; Ha, T.; Weiss, S.; Chemla, D. S. *J. Chem. Phys.* **1999**, *110*, 1195−1201.
(23) Fu, A.; Micheel, C. M.; Cha, J.; Chang, H.; Yang, H.; Alivisatos, A. P. *J. Am. Chem. Soc* **2004**, *126*, 10832−10833.

NL060483Q